Osteoarthritis and Cartilage (2008) **16,** 772–778

doi:10.1016/j.joca.2007.11.004

Osteoarthritis and Cartilage

International Cartilage Repair Society

OARSI OSTEOARTHRITIS RESEARCH SOCIETY INTERNATIONAL

Alteration of *N*-glycans related to articular cartilage deterioration after anterior cruciate ligament transection in rabbits[1]

T. Matsuhashi M.D.†, N. Iwasaki M.D., Ph.D., Associate Professor†*, H. Nakagawa Ph.D., Associate Professor‡, M. Hato‡, M. Kurogochi Ph.D.‡, T. Majima M.D., Ph.D., Associate Professor†, A. Minami M.D., Ph.D., Professor† and S.-I. Nishimura Ph.D., Professor‡

† *Department of Orthopaedic Surgery, Hokkaido University Graduate School of Medicine, Sapporo, Japan*

‡ *Graduate School of Advanced Life Science, Frontier Research Center for Post-Genome Science and Technology, Hokkaido University, Sapporo, Japan*

Summary

Objective: Osteoarthritis (OA) is the most common of all joint diseases, but the molecular basis of its onset and progression is controversial. Several studies have shown that modifications of *N*-glycans contribute to pathogenesis. However, little attention has been paid to *N*-glycan modifications seen in articular cartilage. The goal of this study was to identify disease specific *N*-glycan expression profiles in degenerated cartilage in a rabbit OA model induced by anterior cruciate ligament transection (ACLT).

Methods: Cartilage samples were harvested at 7, 10, 14, and 28 days after ACLT and assessed for cartilage degeneration and alteration in *N*-glycans. *N*-Glycans from cartilage were analyzed by high performance liquid chromatography and mass spectrometry.

Results: Histological analysis showed that osteoarthritic changes in cartilage occurred 10 days after ACLT. Apparent alterations in the *N*-glycan peak pattern in cartilage samples were observed 7 days after ACLT, and overall *N*-glycan changes in OA reflected alterations in both sialylation and fucosylation. These changes apparently preceded histological changes in cartilage.

Conclusion: These results indicate that changes in the expression of *N*-glycans are correlated with OA in an animal model. Understanding mechanisms underlying changes in *N*-glycans seen in OA may be of therapeutic value in treating cartilage deterioration.

Key words: Cartilage, Osteoarthritis, *N*-Glycan.

Introduction

Chondrocyte metabolism is controlled by genetic and environmental factors, such as extracellular matrix (ECM) composition, soluble mediators, or mechanical factors[1,2]. Osteoarthritis (OA), which results from a breakdown in the balance of these factors, is the most common joint disease. To date, numerous studies have investigated its pathogenesis[1–8]. However, factors mediating onset and aggravation of OA are still controversial.

Glycobiology, defined as the analysis of biological function of sugar chains covalently bound to proteins and lipids, has been recently applied to molecular-based investigations[9]. Sugar chains attached to proteins (glycoproteins) and lipids (glycolipids) are commonly referred to as glycans. Glycoprotein glycans are found on the cell surface, in the ECM, and in serum. These glycans act as an interface on the cell surface and modulate protein properties, including folding, secretion, targeting, and protease resistance[10,11]. Several studies show that glycan modifications of proteins contribute to the pathogenesis of some diseases[12,13]. One characteristic of cartilage is that some chondrocytes reside in areas rich in ECM. In addition, it is well known that glycoproteins are abundant on the cell surface and in cartilage ECM. These observations lead to a working hypothesis that sugars attached to proteins contribute to chondrocyte metabolism.

Glycans attached to proteins are classified into two groups: glycans attached to an asparagine residue through a nitrogen atom (*N*-glycans) and those attached to a serine or threonine oxygen (*O*-glycans)[11]. Both types have been intensively studied, and many studies report structural and functional analyses of *N*-glycans[14]. Based on these data, a relationship between *N*-glycan alteration and disease has recently been emerged[12,13,15–18]. For example, several studies of *N*-glycans of serum immunoglobulin G (IgG) molecules associated with the rheumatoid arthritis (RA) indicate that changing *N*-glycan structure contributes to RA[19–21]. However, little attention has been paid to *N*-glycan alterations occurring in articular cartilage in a diseased condition.

Glycans have five major functions: (1) providing cell wall and ECM structural components, (2) modifying protein

[1]Supported by a grant for the National Project on "Functional Glycoconjugate Research Aimed at Developing New Industry" from the Ministry of Education, Science, Sport and Culture of Japan, and SENTAN from the Japan Science and Technology Agency and Uehara Memorial Foundation.

*Address correspondence and reprint requests to: Dr Norimasa Iwasaki, Department of Orthopaedic Surgery, Hokkaido University Graduate School of Medicine, 060-8638, North 15, West 7, Kita-ku, Sapporo, Hokkaido, Japan. Tel: 81-11-706-5936 ext. 5937; Fax: 81-11-706-6054; E-mail: niwasaki@med.hokudai.ac.jp

Received 11 November 2006; revision accepted 17 November 2007.

properties, (3) directing glycoconjugates, (4) mediating and modulating cell adhesion, and (5) mediating and modulating signaling. Thus, we hypothesized that cartilage *N*-glycans would be altered in parallel with cartilage degradation in OA and would vary according to the degree of deterioration. Particularly, *N*-glycan alterations should occur at early phases of OA aggravation. To test this hypothesis, we analyzed *N*-Glycans of rabbit OA cartilage explants induced by anterior cruciate ligament transection (ACLT). The specific aims of this study were to clarify the alterations in cartilage *N*-glycans with OA aggravation and to identify *N*-glycan structures correlated with cartilage deterioration.

Materials and methods

ANIMALS AND SURGICAL PROCEDURES

Seventy-eight adult female Japanese white rabbits (15–16-week-old) weighing 2.6–3.1 kg purchased from a professional breeder (Japan SLC, Inc., Hamamatsu, Japan) were used for this study according to the established ethical guidelines approved by the local animal care committee. Rabbits were anesthetized with 0.6 ml pentobarbital sodium (50 mg/ml) injections and then maintained on isoflurane. To induce osteoarthritic changes of articular cartilage, the right knee ACL was sectioned through a medial parapatellar incision (OA group). As a sham control, arthrotomy without ACLT was performed in sham group. Rabbits were housed in plastic cages and allowed to move freely after the operation. At days 0, 7, 10, 14, and 28, animals were euthanized by an intravenous injection of overdose pentobarbital to obtain cartilage samples for histological and glycostructural analyses. Serum samples were harvested prior to euthanasia. Here, day 7 is defined as 7 days after the operation, and day 0 means the day prior to the operation.

HISTOLOGICAL ANALYSIS ($N = 36$)

To determine osteoarthritic changes in OA and sham groups, cartilage samples ($n = 4$) were analyzed histologically at days 0, 7, 10, 14, and 28. Each sample, including the tibial plateau and femoral condyle, was fixed in 10% neutral buffered formalin. Tissue blocks were decalcified with 14% ethylenediaminetetraacetic acid (EDTA), cut in a sagittal plane, and stained with hematoxylin and eosin (HE) and Safranin O–fast green. To avoid observer bias, slides were coded prior to microscopic analysis. Osteoarthritic changes in each sample were quantified using the modified Mankin score[22].

PREPARATION OF PYRIDYLAMINATED (PA)-*N*-GLYCAN ($N = 42$)

Cartilage samples of the tibial plateau and serum were obtained from each animal at days 0, 7, 10, and 28. Cartilage minced by a razor and serum was heated to 90°C for 15 min. After lyophilization, each sample was digested sequentially with trypsin, chymotrypsin, *N*-glycosidase F, and pronase as described[23]. *N*-Glycan fractions were purified on a gel-filtration column (Bio-Gel P-4, 1×38 cm, water, Nippon Bio-Rad Laboratories KK, Tokyo, Japan), and tagged by fluorescent labeling using 2-aminopyridine to increase sensitivity for analysis[24]. Excess reagents were removed by gel-filtration on Sephadex-G-15 (Amersham Bioscience, Tokyo, Japan). PA-*N*-glycans were analyzed using high performance liquid chromatography (HPLC) and mass spectrometry (MS).

HPLC ANALYSIS

HPLC analysis using the L-7000 HPLC system (Hitachi High-Technologies, Tokyo, Japan) was performed under conditions previously described[25,34,36]. PA-*N*-glycans were separated on an octadecylsilica (ODS) column (HRC-ODS, 6×150 mm, Shimadzu, Kyoto, Japan), and each peak on the ODS column was applied individually to an amide column (TSK-gel Amide-80, 4.6×250 mm, Tosoh, Tokyo, Japan). The relative amount of PA-*N*-glycans was calculated based on the peak area analyzed by attached software on the HPLC system. Elution positions of PA-*N*-glycan on the ODS and amide columns were converted to glucose units (GU), which corresponded to relative degree of polymerization of α1,6-glucose oligosaccharides, for increasing reproducibility. *N*-Glycan structures were suggested by comparing elution positions with data reported in the same analytical conditions, and confirmed with further HPLC analysis combined with partial digestion, and/or MS. Elution positions and code numbers of approximately 500 kinds of oligosaccharide are described in these references[34,35]. The validity of the elution positions and partial digestions was confirmed using well-known standard PA-*N*-glycans and previous studies[27,36].

N-Glycans can form various structures, but have a common core structure and some rules in linkages[11]. To determine the detailed *N*-glycans' structure related to OA, PA-*N*-glycans were digested sequentially with β-*N*-acetylhexosaminidase (HexNAcase, Jack bean, Seikagaku Co., Tokyo, Japan) which removed β-linked GalNAc and GlcNAc, α1,3/4-fucosidase (α3/4-Fase, Takara Co., Shiga, Japan) and weak hydrochloric acid to hydrolyze sialic acids. After each digestion, PA-*N*-glycans were individually analyzed by HPLC on both columns to confirm elution positions[23,25].

MS

To identify the PA-*N*-glycan structure, some PA-*N*-glycans separated by HPLC were further analyzed by matrix-assisted laser desorption/ionization time-of-flight MS (MALDI-TOF MS) using an Ultraflex TOF/TOF mass spectrometer (Bruker Daltonics GmbH, Bremen, Germany). As matrices, 2,5-dehydroxybenzoic acid (DHB) and α-cyano-4-hydroxycinnaminic acid (CHCA) were used. PA-*N*-glycans fractionated on HPLC were dissolved and applied to MALDI-TOF MS as described[26]. Based on results from HPLC and MS, each precise *N*-glycan structure was determined.

All measurements were performed using an Ultraflex TOF/TOF mass spectrometer equipped with a reflector and controlled by the FlexControl 2.2 software package (Bruker Daltonics). In MALDI-TOF MS reflector mode, ions generated by a pulsed UV laser beam (nitrogen laser, $\lambda = 337$ nm, 5 Hz) were accelerated to a kinetic energy of 23.5 kV. Metastable ions generated by laser-induced decomposition of the selected precursor ions were analyzed without any additional collision gas. In MALDI-LIFT-TOF/TOF mode, precursor ions were accelerated to 8 kV and selected in a timed ion gate. The fragments were further accelerated by 19 kV in the LIFT cell (LIFT indicates "lifting" the potential energy for the second acceleration of ion source), and their masses were analyzed after the ion reflector passage. Masses were automatically annotated by using the FlexAnalysis 2.2 software package. External calibration of MALDI mass spectra was carried out using singly charged monoisotopic peaks of a peptide mixture of human angiotensin II (m/z 1046.542), bombesin (m/z 1619.823), ACTH-(18–39) (m/z 2465.199), and somatostatin 28 (m/z 3147.472).

STATISTICAL ANALYSIS

Data were represented as means $\pm$ standard deviation (SD). Significant differences between groups were assessed by unpaired t tests. P-values of less than 0.05 were considered significant.

Results

HISTOLOGICAL FINDINGS

After the operations, rabbits exhibited a normal gait pattern by footprint analysis (data not shown). Also, infections were not seen macroscopically in any knee joint (data not shown). At day 7, no histological changes of the tibial plateau were seen in HE-stained samples of the OA group [Fig. 1(b)]. Samples evaluated at day 10 showed common OA changes, including deterioration of the superficial cartilage layer and a reduced number of chondrocytes in superficial and middle cartilage layers [Fig. 1(c)]. At day 28, a reduced number of chondrocytes were observed in whole layers [Fig. 1(e)], and cloning of chondrocytes was apparent in these damaged areas [Fig. 1(e)]. While Safranin O–fast green staining showed no significant change from day 7 to day 14 [Fig. 1(g–i)], both showed significant reduction at day 28 [Fig. 1(j)]. In the sham group, from day 7 to day 28 no histological indications of OA changes were observed in any samples (data not shown). Histological changes of the femoral condyle were observed later than histological changes of the tibial plateau (data not shown). After day 10, mean histological scores of the tibial plateau were significantly higher in the OA group than in the sham group (3.6 ± 0.5 vs 2.3 ± 0.5 at day 10, $P < 0.05$; 7.0 ± 0.6 vs 2.4 ± 0.4 at day 28, $P < 0.05$, Fig. 2).

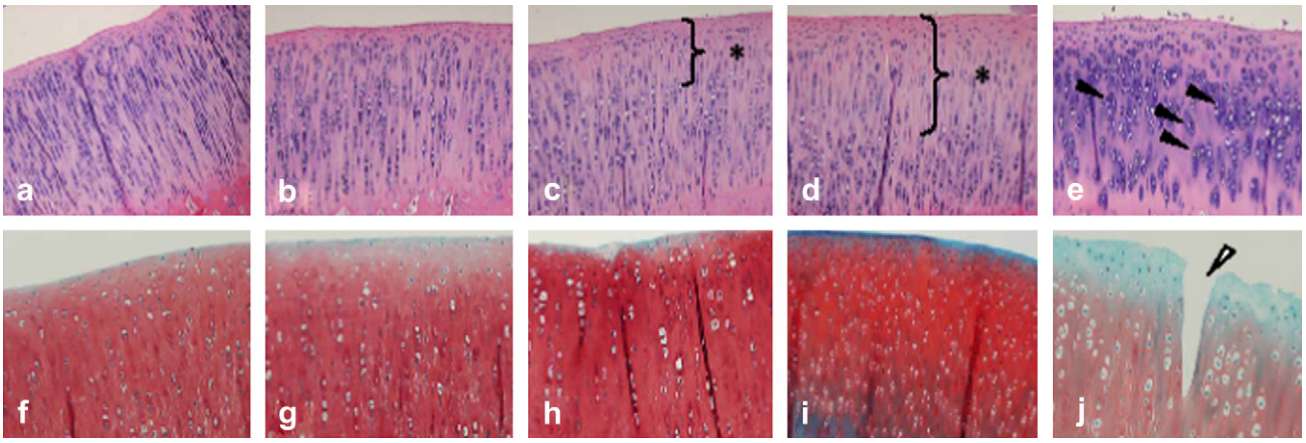

Fig. 1. Histology of cartilage after ACLT in medial tibial plateau in the rabbit knee joint. (a–e) HE-stained sections. (f–j) Safranin O-fast green stained sections. (a) Control articular cartilage shows a smooth surface. (b) At day 7, no significant changes compared with control cartilage were observed. (c) At day 10, superficial diffuse loss of chondrocytes (*) with surface irregularity was observed. (d) At day 14, diffuse loss of chondrocytes from superficial and middle zones (*) with surface irregularity was observed. (e) At day 28, diffuse loss of chondrocytes in the whole zone with clone formation (solid arrow) was observed. (f) Control articular cartilage with Safranin O-fast green stain. (g–i) At days 7,10, and14, no significant change of Safranin O-fast green staining was observed. (j) At day 28, severe loss of Safranin O–fast green staining and clefts (empty arrow) was observed.

ALTERATION IN *N*-GLYCAN PROFILES

We found no significant alterations in the *N*-glycan peak pattern of serum from day 7 to day 28 in the OA group (Fig. 3). In cartilage analysis, there were no apparent alterations in the *N*-glycan peak pattern from day 7 to day 28 in the sham group. By contrast, significant alterations in the *N*-glycan peak pattern in cartilage were observed in the OA group from day 7 postoperatively (Fig. 4). Alterations in peak shape suggested a change in the composition of *N*-glycans contained in the peak. To confirm this, we purified peaks by HPLC on an ODS column and analyzed each on an amide column in a different chromatographic mode. Each altered peak on the ODS column was separated into three peaks on the amide column, referred to as *N*-glycan A (a), B (b), and C (c) in the order of separation time (Fig. 4*). We then calculated each area ratio. The mean ratio of *N*-glycan A in the OA group significantly decreased from day 7 to day 28 compared to the sham group (40.6 ± 1.80 vs 36.0 ± 1.40 at day 7, $P < 0.05$; 39.8 ± 1.54 vs 35.6 ± 1.97 at day 28, $P < 0.05$, Fig. 5), while the value of *N*-glycan C in the OA group significantly increased from day 7 compared to the sham group (44.7 ± 1.91 vs 40.8 ± 1.28 at day 7, $P < 0.05$; 46.0 ± 2.67 vs 40.2 ± 1.03 at day 28, $P < 0.05$, Fig. 5). The mean ratio of *N*-glycan B did not significantly change (data not shown). The mean ratio of *N*-glycans A–C after day 7 was significantly higher in the OA group than in the sham group (1.25 ± 0.11 vs 1.01 ± 0.04 at day 7, $P < 0.05$; 1.32 ± 0.11 vs 1.01 ± 0.04 at day 28, $P < 0.05$, Fig. 5).

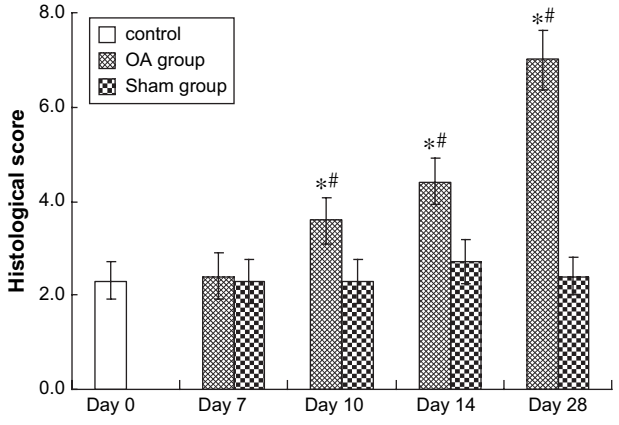

Fig. 2. Histological scores of medial tibial plateau. Values are means ± SD. Shown are scores for histological parameters with comparisons between groups. Histological analysis revealed that slightly degenerative changes in cartilage occurred in all cases starting 10 days after ACLT. *Denotes statistical significance ($P < 0.05$) vs sham group. #Denotes statistical significance ($P < 0.05$) vs control.

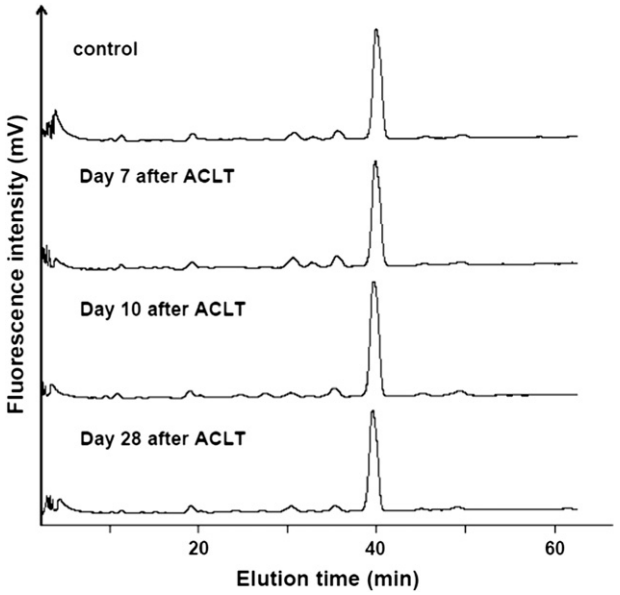

Fig. 3. Chromatograms of PA-*N*-glycans obtained from rabbit serum glycoproteins on an ODS column. There were no significant alterations in the *N*-glycan peak pattern of serum from day 7 to day 28 in the OA group compared with controls.

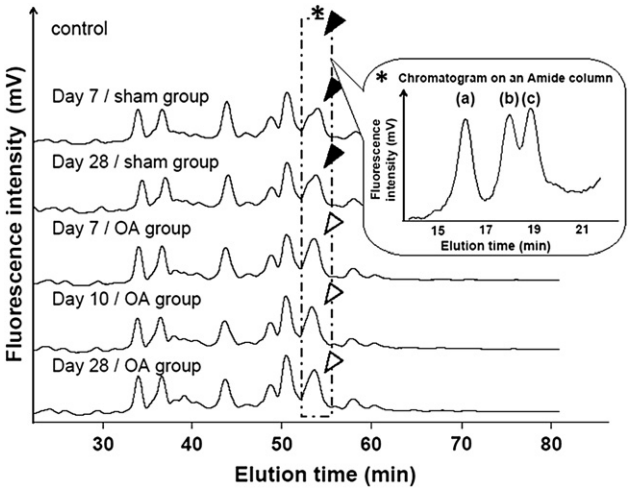

Fig. 4. Chromatograms of PA-*N*-glycans obtained from rabbit cartilage glycoproteins on an ODS column. Two peaks (solid arrow) in the chart of day 0 and the sham-operated group were seen as one peak (empty arrow) from day 7 after ACLT. Those peaks included three peaks on an amide column, referred to as *N*-glycan A (a), B (b), and C (c), in the order of separation time (*).

STRUCTURAL ANALYSIS OF *N*-GLYCANS RELATED TO OSTEOARTHRITIC CHANGES

MALDI-TOF spectra of *N*-glycans A and C with DHB as a matrix indicated a molecular mass of 2239.6 and 2094.6, respectively (Fig. 6). Each MALDI-TOF/TOF spectra showed constituents of *N*-glycans A and C (Fig. 7). MALDI-TOF and TOF/TOF spectra of *N*-glycans with CHCA as a different matrix indicated almost the same mass fragmentation compared with DHB (data not shown). Molecular mass of 2239.6 and 2094.6 corresponds with a protonated PA-glycan which consists of 3 Hex, 6 HexNAc and *N*-acetylneuraminic acid (NANA); and 3 Hex, 6 HexNAc and Fuc, respectively. These compositions and abundant fragment peaks of di-HexNAc (406.9 and 407.1) and peaks devoid of di-HexNAc, 1542.1 and 1542.2, indicate these *N*-glycans which include GalNAc–GlcNAc units instead of Gal–GlcNAc units in their outer arms. After sequential partial digestion, elution positions of both *N*-glycans on the two-dimensional map coincided with 110.4a GalNAcβ1,4-GlcNAcβ1,2-Manα1,3-(Manα1,6-)Manβ1,4-GlcNAcβ1,4-(Fucα1,6-)GlcNAc which confirmed from a previous study combining HPLC, NMR and methylation analyses[31]. The elution position on the amide column was smaller than the one of a similar structure, 110.4, which includes Galβ1,4–GlcNAc units in their outer arms[25]. Based on these results, the final form of *N*-glycan digested partially was assigned as 110.4a, and elution positions and suggested structures of digested *N*-glycans A and C are shown in Fig. 8. This indicated that NANA of *N*-glycan A and Fuc of *N*-glycan C was attached to the same α3Man branch of the outer arm and di-HexNAc is GalNAcβ1,4–GlcNAc[31]. The NANA to GalNAc linkage was determined to be α2,6 based on an observed reduction in GU on the amide column[27]. α2,3 NeuAc was reduced to about 0.5 GU on the amide column; on the other hand α2,6 NeuAc increased by about 0.2 GU on the amide column according to the two-dimensional mapping technique[32,33]. The linkage of Fuc in the outer arm of *N*-glycan C was determined to be

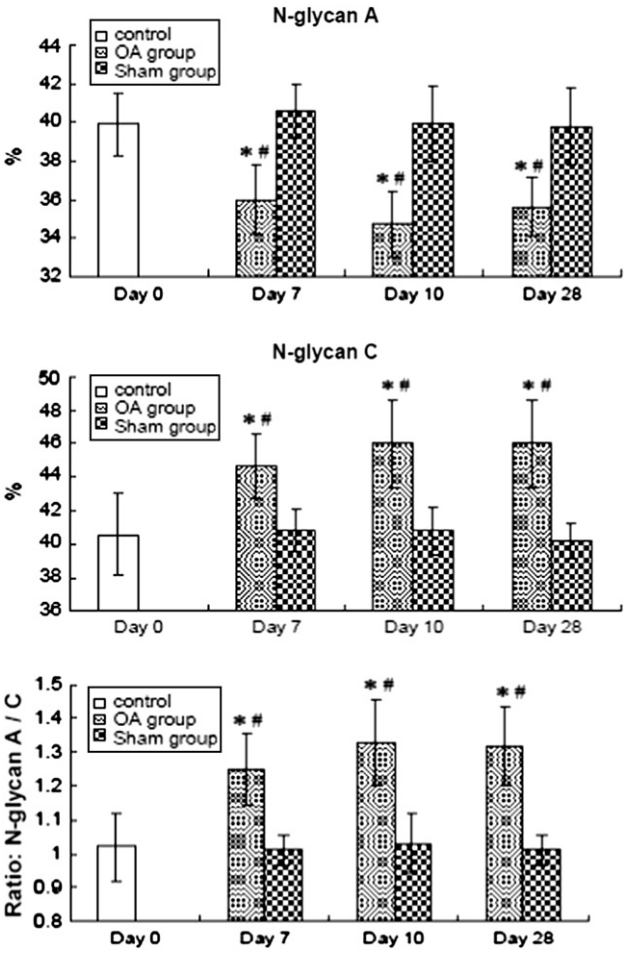

Fig. 5. The ratio in the peak area of *N*-glycans related to OA. Values are means ± SD. The mean ratio of *N*-glycan A decreased significantly from 7 days in the OA group. The mean ratio of *N*-glycan C increased significantly from 7 days in the OA group. The mean ratio of *N*-glycan A–C increased significantly from 7 days in the OA group. *Denotes statistical significance ($P < 0.05$) vs sham group. #Denotes statistical significance ($P < 0.05$) vs control.

an α1,3 linkage to GlcNAc because it was digested with α3/4-Fase and the GalNAc bound to 4 position of GlcNAc. Changing of elution positions with partial digestion is already confirmed in a previous report[32,33]. In this way, structures of *N*-glycans A and C were finally determined as in Fig. 9.

Discussion

The goal of this study was to determine potential alterations in cartilage *N*-glycans with aggravated OA. We first showed alterations in the *N*-glycan peak pattern of articular cartilage between normal rabbit cartilage (sham group) and OA cartilage induced by ACLT (OA group). Then, by comparing peaks obtained from both groups, we showed that the composition of cartilage *N*-glycans was significantly altered in the OA group prior to apparent histological changes. This observation indicates that *N*-glycan alterations in cartilage occur at very early phases of OA aggravation. It is well known that alterations in *N*-glycans are associated with specific disease-related mechanisms[12,13,15]. Several studies of rheumatic diseases report

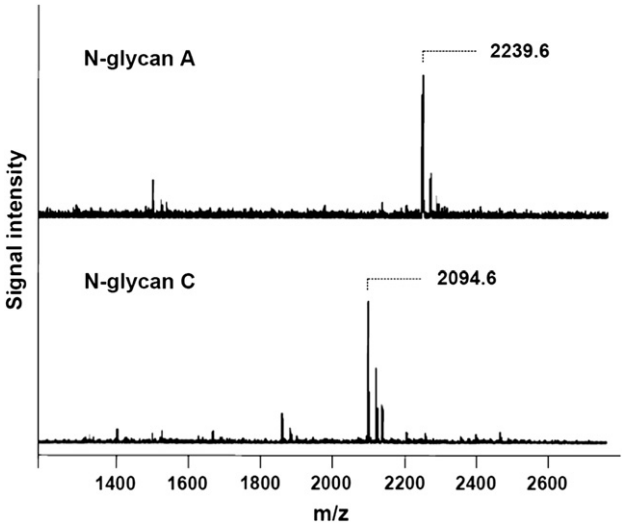

Fig. 6. MALDI-TOF mass spectra. Mass spectrometric analysis of *N*-glycans A and C by the MALDI-TOF/TOF method using DHB as a matrix.

alterations in the *N*-glycan pattern of serum IgG[19–21]. However, little attention has been given to similar alterations in articular cartilage. OA, a chronic degenerative joint disease characterized by articular cartilage deterioration and damage to subchondral bone, is a major cause of disabilities affecting patients' daily activities. Unlike RA, OA is primarily considered a local disease caused by abnormal loading on the articular cartilage. Therefore, analysis of cartilage *N*-glycans may facilitate the understanding of OA pathogenesis. To our knowledge, this is the first study to determine the structure of cartilage *N*-glycans and show alterations in the composition of the cartilage *N*-glycans with OA aggravation.

In early stages of OA aggravation, the macromolecular structure of the ECM is disrupted[5]. Early in this process, chondrocytes begin secreting enzymes that can disrupt ECM macromolecules[1,2]. In particular these enzymes decrease proteoglycan aggregation and concentration of

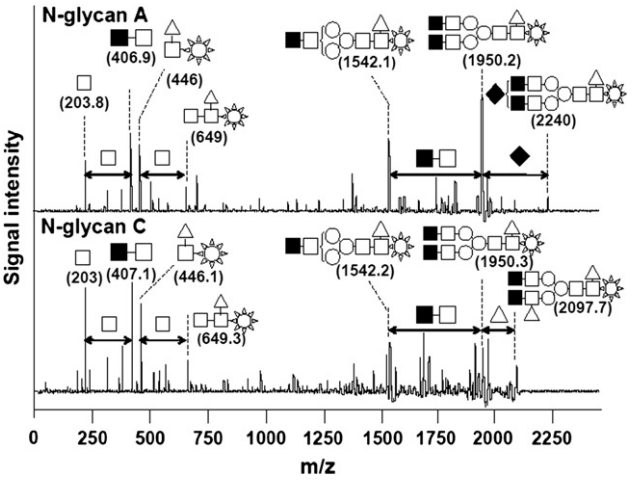

Fig. 7. MALDI-TOF/TOF mass spectra. Structural analysis of *N*-glycans A and C by the MALDI-TOF/TOF method using DHB as a matrix. Structures of fragments of *N*-glycan in each peak are indicated. Mannose, ○; Fuc, △; GalNAc, ■; GlcNAc, □; NANA, ◆; PA, ☼.

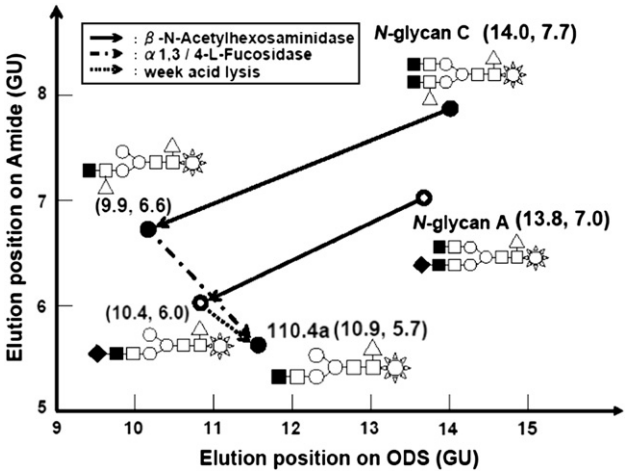

Fig. 8. Structural characterization of *N*-glycans A and C by a combination of exoglycosidase digestion and two-dimensional mapping. A portion of *N*-glycans A and C was digested with exoglycosidases. The elution times on ODS and amide-silica columns of *N*-glycans and their exoglycosidase digests are plotted on a two-dimensional sugar map (expressed as GU). Arrows indicate the direction of changes in the coordinates of *N*-glycans A and C after digestion with: → β-*N*-acetylhexosaminidase, ⋯▸ α1,3/4-fucosidase, -▸ weak acid lysis.

cartilage ECM, and their release is accompanied by an increased rate of chondrocyte apoptosis in areas of cartilage regeneration. Our analysis indicates that cartilage *N*-glycans undergo changes in the early phases of OA aggravation. *N*-glycans are abundant on the cell surface and in the ECM, and they commonly interact with protein receptors known as lectins. Through this interaction, *N*-glycans mediate cell–cell and cell–ECM interactions and intra- and extracellular signaling. The current study showed alteration in the representation of two kinds of *N*-glycan whose branch has sialic acid and fucose. Although we suppose that these *N*-glycans relate to OA initiation or progression in early phase, their biological functions remain unclear. Further studies will be performed to elucidate their functional roles in OA progression. Therefore, alterations in the composition of 1A1-210.4b (*N*-glycan A) and 210.41b (*N*-glycan C), whose structures are identified here, likely play crucial roles in the response of chondrocytes or

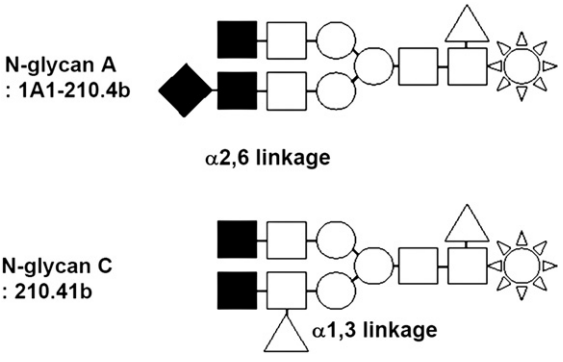

Fig. 9. Structure of *N*-glycans A and C. Indicated are structures of *N*-glycans related to OA. Mannose, ○; Fuc, △; GalNAc, ■; GlcNAc, □; NANA, ◆; PA ☼.

the ECM to changes in the cartilage environment responsible for initiating OA. Here, we did not identify the localization of these *N*-glycans. Future studies are required to determine the biological roles of *N*-glycans identified here in early phases of OA. We observed no significant alterations in the serum *N*-glycan pattern with OA aggravation. Watson *et al.*[20], however, showed alterations in the *N*-glycan pattern of serum IgG with rheumatic diseases, including RA, systemic lupus erythematosus, ankylosing spondylitis, Sjögren's disease, juvenile chronic arthritis, and psoriatic arthritis. In addition to RA, Parekh *et al.*[21] analyzed the *N*-glycan pattern of serum IgG in patients with primary OA and showed that IgG isolated from patients with primary OA contained different distributions of bi-antennary complex-type *N*-glycans. They concluded that primary OA may be a disease related to changes in intracellular processing of *N*-glycans or in their post-secretory degradation. Differences between their results and ours may be due to differences in the *N*-glycan source, to serum or purified IgG, or to mechanisms that induce OA disease. Our current model is a secondary OA model, in which disease is caused by joint instability. Pathological changes must be localized in tissues constituting the joint with cartilage deterioration. Therefore, we conclude that alterations in the *N*-glycan pattern occur in cartilage, not in serum. The results obtained from analysis of both serum and cartilage confirm that OA aggravation following joint instability mainly results from local pathogenesis.

These results and analytical methods can now be applied to clinical studies. The *N*-glycan pattern of articular cartilage may be used as a diagnostic indicator of OA or a predictable indicator of disease aggravation. Although we focus on early phases of OA aggravation, the *N*-glycan pattern of articular cartilage obtained from rheumatic diseases and at advanced stages of OA should now be addressed. By comparing these results, the utility of the *N*-glycan pattern as disease indicators will be established. Also, it is likely that 1A1-210.4b (*N*-glycan A) and 210.41b (*N*-glycan C) identified here play crucial roles in regulating cartilage deterioration following joint instability, but the localization and functional roles of these *N*-glycans are unknown. We are now determining the identities of proteins with specific *N*-glycan structures. When that analysis is complete, we will use knock-out or knock-down of either glycosyltransferase genes or the carrying proteins, followed by a functional analysis of *N*-glycans to further analyze their roles in cartilage deterioration. Finally, the *N*-glycan pattern likely depends on species. For this analysis we used rabbit cartilage, but *N*-glycans altered in human OA cartilage may differ from the *N*-glycans identified here. Thus, the *N*-glycan pattern of degenerative articular cartilage in humans will be analyzed in future studies.

Based on results presented here, we predict that *N*-glycans of human cartilage will alter with cartilage deterioration in diseases such as OA and RA. We will likely observe changes in the linkage of saccharides such as sialic acid and fucose, which is attached to the outer arm of *N*-glycan. Complex combinations of glycosyltransferases and glycosidases control *N*-glycan composition. Therefore, further analysis of expression of glycosyltransferases and glycosidases related to cartilage *N*-glycans should lead to elucidation of the pathogenesis of these diseases.

Regarding the biological and biochemical functions of *N*-glycans obtained in this study, we cannot study any further rabbit model. The reason is that DNA sequences of glycosyltransferases and glycosidases related with cartilage *N*-glycans of rabbit are little known. In our future studies, using human cartilages and conditional model mice, we should determine the functional roles of the *N*-glycans. This should lead to a novel strategy for the treatment of OA.

Recent studies suggest that changes in glycosylation, defined as the addition of sugars to proteins and lipids, have a direct role in the etiology of various diseases, including congenital disorders of glycosylation, von Willebrand factor deficiency, rheumatic diseases, cancers, and emphysema[12,13,19,20,28–30]. Regarding joint diseases, ours is the first study to determine the structure of the cartilage *N*-glycans and analyze potential alterations in damaged cartilage and may provide diagnostics and further insight into OA pathogenesis.

Conflict of interest

The authors have no conflict of interest.

Acknowledgments

We thank Ms Satomi Kudo very much for excellent technical assistance.

References

1. Goldring MB. The role of the chondrocyte in osteoarthritis. Arthritis Rheum 2000;43:1916–26.
2. Bluteau G, Conrozier T, Mathieu P, Vignon E, Herbage D, Mallein-Gerin F. Matrix metalloproteinase-1, -3, -13 and aggrecanase-1 and -2 are differentially expressed in experimental osteoarthritis. Biochim Biophys Acta 2001;1526:147–58.
3. Hamerman D. Aging and osteoarthritis: basic mechanism. J Am Geriatr Soc 1993;4:760–70.
4. Quasnichka HL, Anderson-MacKenzie JM, Tarlton JF, Sims TJ, Billingham ME, Bailey AJ. Cruciate ligament laxity and femoral intercondylar notch narrowing in early-stage knee osteoarthritis. Arthritis Rheum 2005;52:3100–9.
5. Malfait AM, Liu RQ, Ijiri K, Komiya S, Tortorella MD. Inhibition of ADAM-TS4 and ADAM-TS5 prevents aggrecan degradation in osteoarthritic cartilage. J Biol Chem 2002;277:22201–8.
6. Dai SM, Shan ZZ, Nakamura H, Masuko-Hongo K, Kato T, Nishioka K, *et al.* Catabolic stress induces features of chondrocyte senescence through overexpression of caveolin 1: possible involvement of caveolin 1-induced down-regulation of articular chondrocytes in the pathogenesis of osteoarthritis. Arthritis Rheum 2006; 54:818–31.
7. Kouri JB, Rojas L, Perez E, Abbud-Lozoya KA. Modifications of Golgi complex in chondrocytes from osteoarthritic (OA) rat cartilage. J Histochem Cytochem 2002;50:1333–40.
8. Bluteau G, Gouttenoire J, Conrozier T, Mathieu P, Vignon E, Richard M, *et al.* Differential gene expression analysis in a rabbit model of osteoarthritis induced by anterior cruciate ligament (ACL) section. Biorheology 2002;39:247–58.
9. Varki A. Biological roles of oligosaccharides: all of the theories are correct. Glycobiology 1993;3:97–130.
10. Wong CH. Protein glycosylation: new challenges and opportunities. J Org Chem 2005;70:4219–25.
11. Kobata A. Structure and function of the sugar chains of glycoprotein. Eur J Biochem 1992;209:483–501.
12. Yamashita K, Ideo H, Ohkura T, Fukushima K, Yuasa I, Ohno K, *et al.* Sugar chains of serum transferrin from patients with carbohydrate deficient glycoprotein syndrome. Evidence of asparagine-N-linked oligosaccharide transfer deficiency. J Biol Chem 1993;268:5783–9.
13. Wang X, Inoue S, Gu J, Miyoshi E, Noda K, Li W, *et al.* Dysregulation of TGF-β1 receptor activation leads to abnormal lung development and emphysema-like phenotype in core fucose-deficient mice. Proc Natl Acad Sci U S A 2005;102:15791–6.
14. Wacker M, Linton D, Hitchen PG, Nita-Lazar M, Haslam SM, North SJ, *et al.* N-linked glycosylation in *Campylobacter jejuni* and its functional transfer into *E. coli*. Science 2002;298:1790–3.
15. Jaeken J, Carchon H. Congenital disorders of glycosylation: the rapidly growing tip of the iceberg. Curr Opin Neurol 2001;14:811–5.
16. Landberg E, Pahlsson P, Lundblad A, Arnetorp A, Jeppsson JO. Carbohydrate composition of serum transferrin isoforms from patients

with high alcohol consumption. Biochem Biophys Res Commun 1995; 210:267–74.
17. Reitter JN, Means RE, Desrosiers RC. A role for carbohydrates in immune evasion in AIDS. Nat Med 1998;4:679–84.
18. Xiping W, Julie MD, Shuyi W, Huxiong H, John CK, Xiaoyun W, *et al*. Antibody neutralization and escape by HIV-1. Nature 2003;422:307–12.
19. Chou CT. Binding of rheumatoid and lupus synovial fluids and sera-derived human IgG rheumatoid factor to degalactosylated IgG. Arch Med Res 2002;33:541–4.
20. Watson M, Rudd PM, Bland M, Dwek RA, Axford JS. Sugar printing rheumatic diseases: a potential method for disease differentiation using immunoglobulin G oligosaccharides. Arthritis Rheum 1999;42: 1682–90.
21. Parekh RB, Dwek RA, Sutton BJ, Fernandes DL, Leung A, Stanworth D, *et al*. Association of rheumatoid arthritis and primary osteoarthritis with changes in the glycosylation pattern of total serum IgG. Nature 1985; 316:452–7.
22. Tiraloche G, Girard C, Chouinard L, Sampalis J, Moquin L, Ionescu M, *et al*. Effect of oral glucosamine on cartilage degradation in a rabbit model of osteoarthritis. Arthritis Rheum 2005;52: 1118–28.
23. Nakagawa H, Kawamura Y, Kato K, Shimada I, Arata Y, Takahashi N. Identification of neutral and sialyl N-linked oligosaccharide structures from human serum glycoproteins using three kinds of high-performance liquid chromatography. Anal Biochem 1995;226:130–8.
24. Hase S, Ikenaka T, Matsushima Y. Structure analyses of oligosaccharides by tagging of the reducing end sugars with a fluorescent compound. Biochem Biophys Res Commun 1978;85:257–63.
25. Tomiya N, Awaya J, Kurono M, Endo S, Arata Y, Takahashi N. Analyses of N-linked oligosaccharides using a two-dimensional mapping technique. Anal Biochem 1988;171:73–90.
26. Kurogochi M, Nishimura S-I. Structural characterization of glycopeptides by matrix-dependent selective fragmentation of MALDI-TOF/TOF tandem mass spectrometry. Anal Chem 2004;76:6097–101.
27. Takahashi N, Nakagawa H, Fujikawa K, Kawamura Y, Tomiya N. Three-dimensional elution mapping of pyridylaminated N-linked neutral and sialyl oligosaccharides. Anal Biochem 1995;226: 139–46.
28. Sakuma K, Fujimoto I, Hitoshi S, Tanaka F, Ikeda T, Tanabe K, *et al*. An *N*-glycan structure correlates with pulmonary metastatic ability of cancer cells. Biochem Biophys Res Commun 2006;340:829–35.
29. Peracaula R, Tabares G, Royle L, Harvey DJ, Dwek RA, Rudd PM, *et al*. Altered glycosylation pattern allows the distinction between prostate-specific antigen (PSA) from normal and tumor origins. Glycobiology 2003;13:457–70.
30. Mohlke KL, Purkayastha AA, Westrick RJ, Smith PL, Petryniak B, Lowe JB, *et al*. Mvwf, a dominant modifier of murine von Willebrand factor, results from altered lineage-specific expression of a glycosyltransferase. Cell 1999;96:111–20.
31. Tomiya N, Awaya J, Kurono M, Hanazawa H, Shimade I, Arata Y, *et al*. Structural elucidation of a variety of GalNAc-containing N-linked oligosaccharides from human urinary kallidinogenase. J Biol Chem 1993;268:113–26.
32. Tomiya N, Takahashi N. Contribution of component monosaccharides to the coordinates of neutral and sialyl pyridylaminated *N*-glycans on a two-dimensional sugar map. Anal Biochem 1998;264: 204–10.
33. Takahashi N, Wada Y, Awaya J, Kurono M, Tomiya N. Two-dimensional elution map of GalNAc-containing N-linked oligosaccharides. Anal Biochem 1993;208:96–109.
34. Takahashi N, Tomiya N. Analysis of N-linked oligosaccharides: application of glycoamidase A. In: Muramatsu T, Takahashi N, Eds. Handbook of endoglycosidases and glycoamidases. Boca Raton: CRC Press; 1992: 199–332.
35. <http://www.glycoanalysis.info/>; 1992.
36. Nakagawa H, Deguchi K. Structural analysis of sialyl *N*-glycan using pyridylamination and chromatography followed by multistage tandem mass spectrometry. In: Fukuda M, Ed. Methods in Enzymology. San Diego: Elsevier 2006;415:87–104.